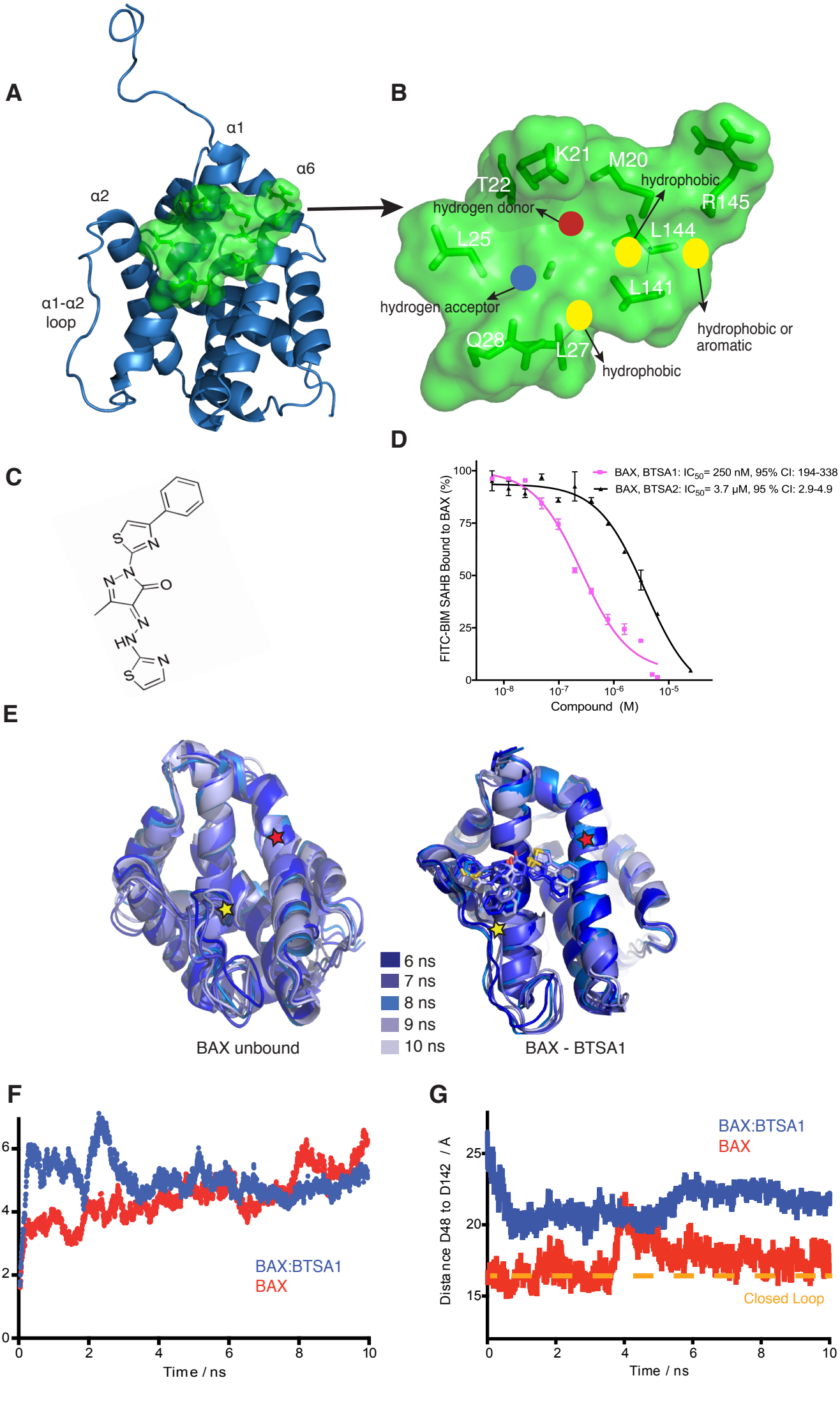
A
α1
α6
α2
α1-α2
loop
B
K21
M20
hydrophobic
T22
R145
hydrogen donor
L144
L25
L141
hydrogen acceptor
hydrophobic or
aromatic
Q28
L27
hydrophobic
C
D
BAX, BTSA1: IC50= 250 nM, 95% CI: 194-338
BAX, BTSA2: IC50= 3.7 μM, 95 % CI: 2.9-4.9
FITC-BIM SAHB Bound to BAX (%)
100
75
50
25
0
10-8
10-7
10-6
10-5
Compound (M)
E
6 ns
7 ns
8 ns
9 ns
10 ns
BAX unbound
BAX - BTSA1
F
Backbone RMSD / Å
6
4
2
0
BAX:BTSA1
BAX
0
2
4
6
8
10
Time / ns
G
Distance D48 to D142 / Å
25
20
15
BAX:BTSA1
BAX
Closed Loop
0
2
4
6
8
10
Time / ns

Figure S1. Related to Figure 1.

A pharmacophore model for the discovery of BTSA1 and validation of its bound orientation that is consistent with BTSA1 keeping the BAX α1-α2 loop in an open conformation. (A) A ribbon representation of the BAX structure highlighting the surface (green) that includes the core BAX trigger site on the structure of BAX. **(B)** A pharmacophore model that was used for the identification of BTSA1 in zoomed view of the core BAX trigger site surface (green). The pharmacophore model contains the following five requirements: a hydrogen bond acceptor for interaction with residue Q28, a hydrogen bond donor for interaction with residue K21, a hydrophobic group for interaction with residue L27, a hydrophobic group for interaction with residue L141 or M20 and a hydrophobic or aromatic group for interaction with residue L144. **(C)** Chemical structure of BTSA2. A methyl is attached to the pyrazolone group for BTSA2 instead of a phenyl group for BTSA1 **(D)** Competitive fluorescence polarization binding assay of BTSA1 and BTSA2 using fluorescent-labeled FITC-BIM $SAHB_{A2}$ bound to BAX. Data are presented as mean ± SD from duplicates of two independent experiments. (**E**) Overlay of the structures from the unbound BAX MD simulation (left) and the BTSA1-bound BAX MD simulation (right) taken from the 6 ns, 7 ns, 8 ns, 9 ns, 10 ns time points. **(F)** Plot of the root square mean deviation over the backbone of BAX residues from the calculated structures of the MD simulations as a function of the time demonstrated the equilibration process of the two simulations. **(G)** The conformation of α1-α2 loop was calculated based on the distance between backbone N atoms of D48 residue of the α1-α2 loop and D142 of the α6 helix. The plot shows the D48-D142 distance over the time of the MD simulations. The D48-D142 distance in the inactive and closed loop conformation of the average calculated NMR structure is shown with orange dotted line. The α1-α2 loop in closed (BAX unbound) and open conformations (BTSA1-BAX) are also shown in the structural overlays in **E**. The position of the D48 and D142 is shown with yellow and red asterisks respectively.

A

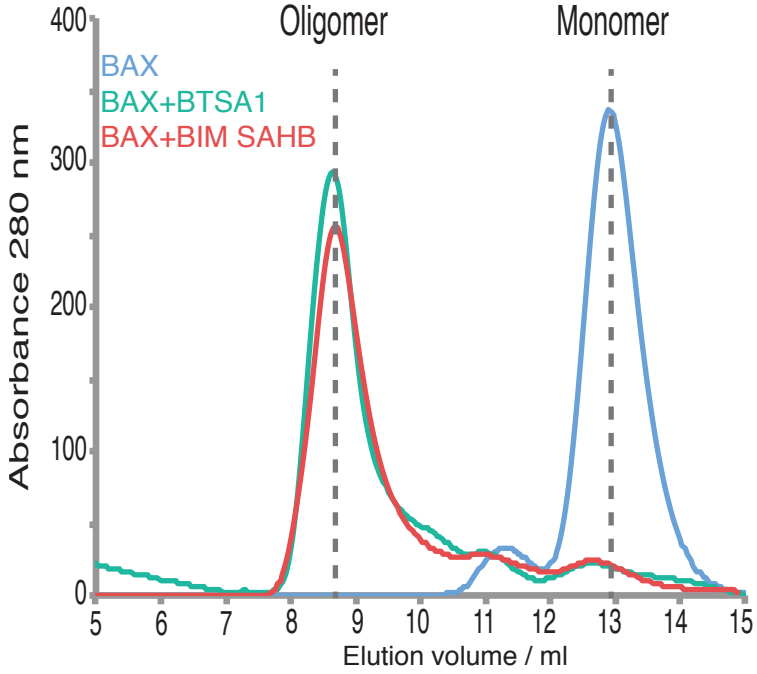
Oligomer
Monomer
BAX
BAX+BTSA1
BAX+BIM SAHB
Absorbance 280 nm
400
300
200
100
0
5
6
7
8
9
10
11
12
13
14
15
Elution volume / ml

B

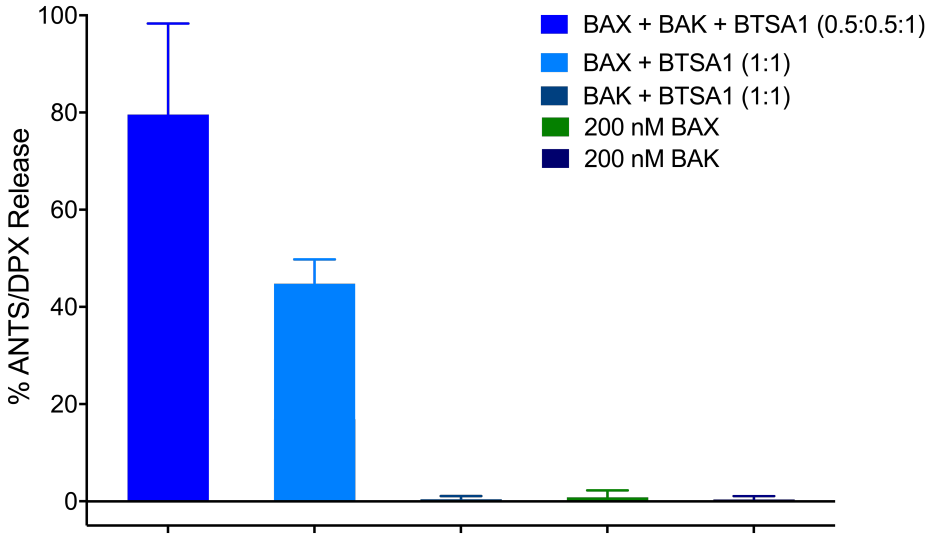
BAX + BAK + BTSA1 (0.5:0.5:1)
BAX + BTSA1 (1:1)
BAK + BTSA1 (1:1)
200 nM BAX
200 nM BAK
% ANTS/DPX Release
100
80
60
40
20
0

C

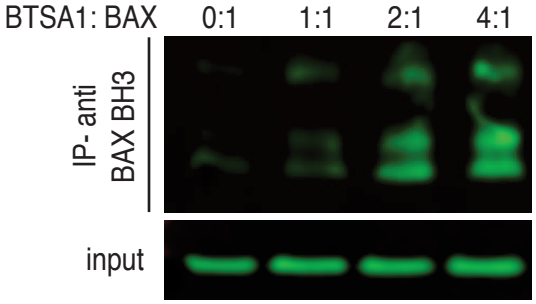
BTSA1: BAX
0:1
1:1
2:1
4:1
IP- anti BAX BH3
input

Figure S2. Related to Figure 2.

BTSA1 induced BAX oligomerization, membrane translocation and BAX-mediated membrane permeabilization but does not directly activate BAK. (A) Size-exclusion chromatography using a SD75 gel filtration column of BAX, BTSA1-treated BAX and BIM $SAHB_{A2}$-treated BAX. (**B**) Liposomal permeabilization assay using 200 nM BAX, 200 nM BAK or 100 nM BAX and 100 nM BAK together upon 200 nM BTSA1 treatment. (**C**) Immunoprecipitation assay using a BAX BH3 domain specific antibody of samples containing 200 nM BAX treated with increasing doses of BTSA1 (200-800 nM) were analyzed by anti-BAX western blot. Data represent mean ± SD (n=3) from two independent experiments or are representative of three independent experiments.

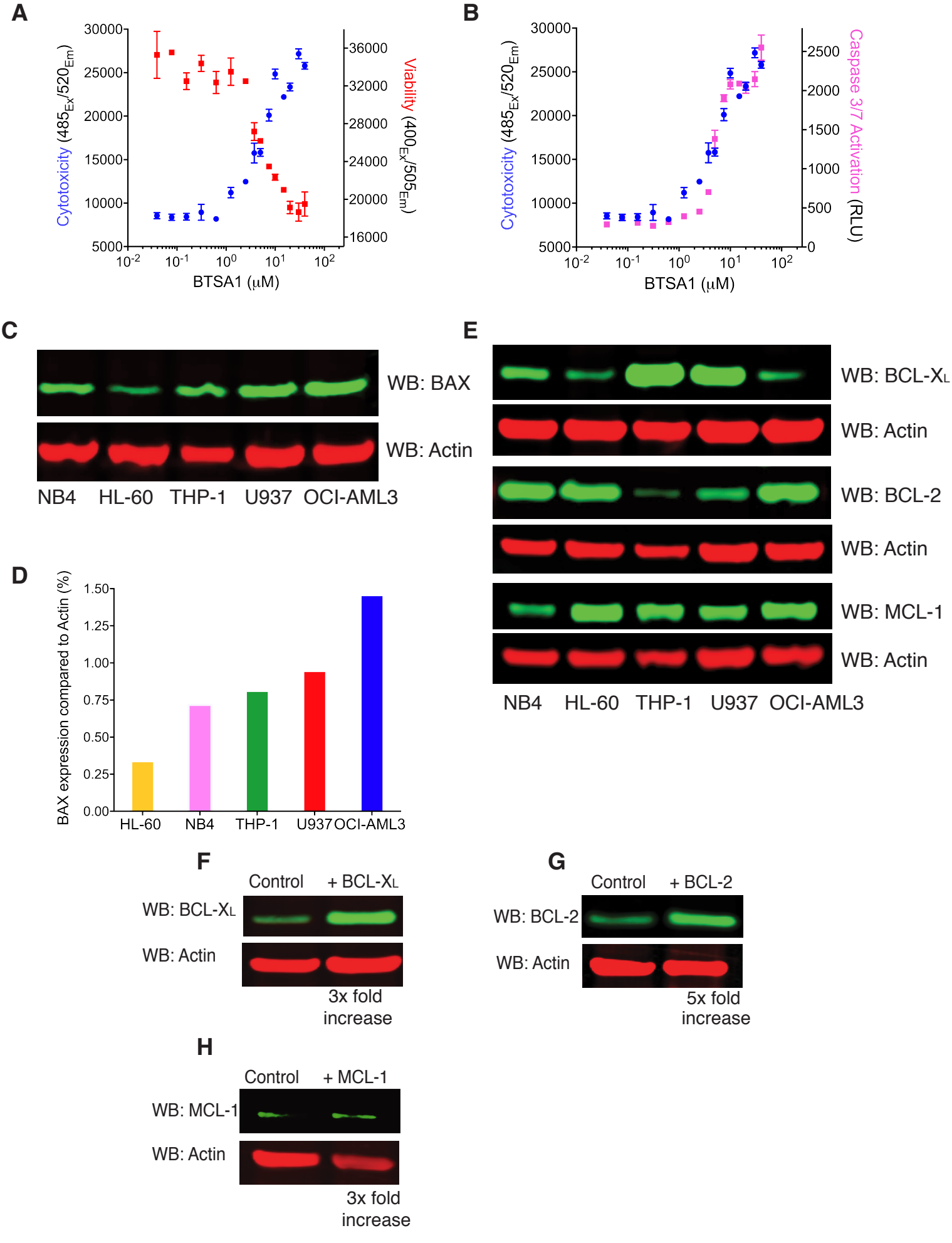
A
Cytotoxicity (485Ex/520Em)
Viability (400Ex/505Em)
BTSA1 (μM)
B
Cytotoxicity (485Ex/520Em)
Caspase 3/7 Activation (RLU)
BTSA1 (μM)
C
WB: BAX
WB: Actin
NB4 HL-60 THP-1 U937 OCI-AML3
D
BAX expression compared to Actin (%)
HL-60 NB4 THP-1 U937 OCI-AML3
E
WB: BCL-XL
WB: Actin
WB: BCL-2
WB: Actin
WB: MCL-1
WB: Actin
NB4 HL-60 THP-1 U937 OCI-AML3
F
Control + BCL-XL
WB: BCL-XL
WB: Actin
3x fold increase
G
Control + BCL-2
WB: BCL-2
WB: Actin
5x fold increase
H
Control + MCL-1
WB: MCL-1
WB: Actin
3x fold increase

Figure S3. Related to Figure 3.

Comparison of cell death assays and quantification of expression levels of BAX, BCL-2, BCL-X_L and MCL-1 for the indicated AML cell line. (A) Comparison of cytotoxicity and viability assay of OCI-AML3 cells treated for 24 hr with increasing concentrations of BTSA1. (**B**) Comparison of cytotoxicity and caspase 3/7 activation assay of OCI-AML3 cells treated for 24 hr with increasing concentrations of BTSA1. **(C)** Western blot analysis using IR fluorescence detection of total BAX and Actin for AML cell lines. **(D)** Percent BAX protein expression levels relative to Actin as measured by quantitative IR fluorescence western for five AML cell lines. **(E)** Western blot analysis using IR fluorescence detection of total BCL-2, BCL-X_L and MCL-1 and Actin for the five AML cell lines. (**F-H**) Western blot analysis using IR fluorescence detection of total BCL-2 (**F**), BCL-X_L (**G**), MCL-1 (**H**) and Actin in NB4 cells before and after transient expression of BCL-2, BCL-X_L and MCL-1 as indicated. The indicated fold of expression change is based on quantification of the IR fluorescence detection for each protein compared to Actin before and after transfection. Data represent mean ± SD (n=3) from two independent experiments or are representative of two independent experiments.

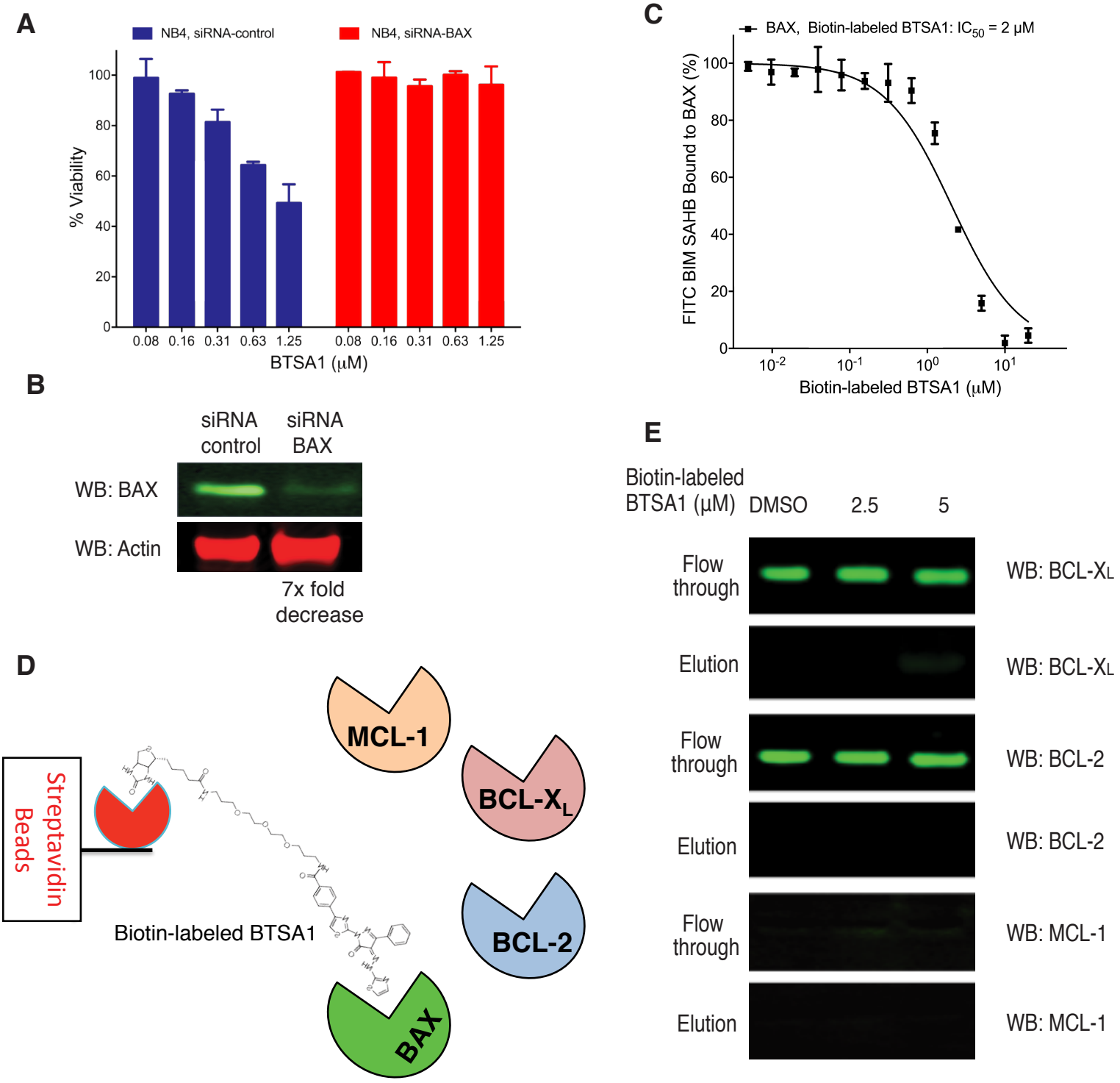
A
NB4, siRNA-control
NB4, siRNA-BAX
% Viability
100
80
60
40
20
0
0.08 0.16 0.31 0.63 1.25
0.08 0.16 0.31 0.63 1.25
BTSA1 (μM)
C
BAX, Biotin-labeled BTSA1: IC50 = 2 μM
FITC BIM SAHB Bound to BAX (%)
100
80
60
40
20
0
10-2
10-1
100
101
Biotin-labeled BTSA1 (μM)
B
siRNA control
siRNA BAX
WB: BAX
WB: Actin
7x fold decrease
E
Biotin-labeled BTSA1 (μM)
DMSO
2.5
5
Flow through
WB: BCL-XL
Elution
WB: BCL-XL
Flow through
WB: BCL-2
Elution
WB: BCL-2
Flow through
WB: MCL-1
Elution
WB: MCL-1
D
Streptavidin Beads
Biotin-labeled BTSA1
MCL-1
BCL-XL
BCL-2
BAX
F
BTSA1 (μM):
0
2.5
5
10
20
1 μM STS
WB: BAX
Cytosol
WB: BAX
Mitochondria
WB: Actin
Cytosol
WB: VDAC
Mitochondria

G

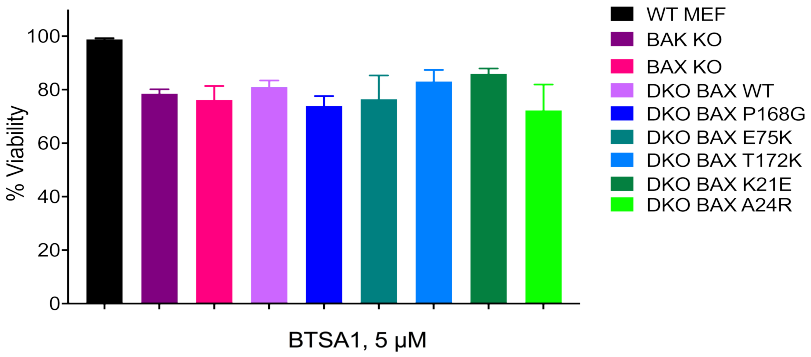
% Viability
100
80
60
40
20
0
BTSA1, 5 μM
WT MEF
BAK KO
BAX KO
DKO BAX WT
DKO BAX P168G
DKO BAX E75K
DKO BAX T172K
DKO BAX K21E
DKO BAX A24R

H

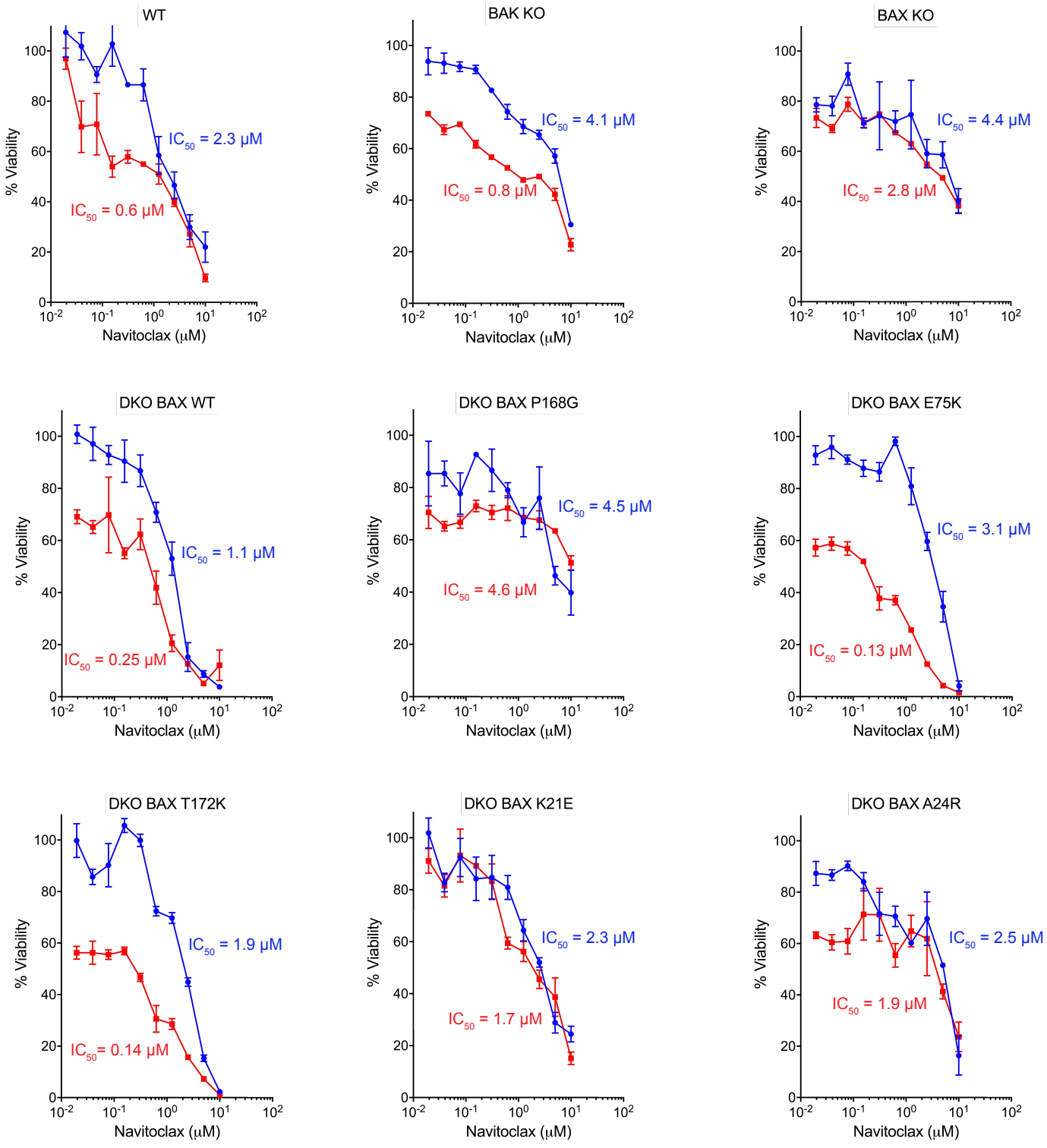
WT
IC50 = 2.3 μM
IC50 = 0.6 μM
BAK KO
IC50 = 4.1 μM
IC50 = 0.8 μM
BAX KO
IC50 = 4.4 μM
IC50 = 2.8 μM
DKO BAX WT
IC50 = 1.1 μM
IC50 = 0.25 μM
DKO BAX P168G
IC50 = 4.5 μM
IC50 = 4.6 μM
DKO BAX E75K
IC50 = 3.1 μM
IC50 = 0.13 μM
DKO BAX T172K
IC50 = 1.9 μM
IC50= 0.14 μM
DKO BAX K21E
IC50 = 2.3 μM
IC50 = 1.7 μM
DKO BAX A24R
IC50 = 2.5 μM
IC50 = 1.9 μM
% Viability
Navitoclax (μM)

Figure S4. Related to Figure 4.

Biochemical data demonstrate specificity of BTSA1 to engage BAX in cells. (A) Viability assay of BTSA1-treated NB4 cells for 24 hr after silencing of BAX expression using siRNA BAX. (**B**) Western blot analysis using IR fluorescence detection of total BAX and Actin in NB4 cells before and after transient treatment with siRNA BAX. The indicated fold of expression change is based on quantification of the IR fluorescence detection for each protein compared to Actin before and after transfection. **(C)** Biotin-labeled BTSA1 displaced fluorescein-labeled FITC-BIM $SAHB_{A2}$ from the BAX trigger site of BAX with an IC_{50} of 2 μM using a competitive fluorescence polarization assay. (**D**) Schematic of the structure of biotin-labeled BTSA1 and pull down experiment performed in OCI-AML3 cells. **(E)** Pull down experiment using biotin-labeled BTSA1 loaded to streptavidin beads followed by western blot analysis with anti-BCL-2, anti-BCl-X_L and anti-MCL-1 antibodies. Flow-through of unbound proteins is shown to confirm protein levels. (**F**) MEF cells treated with (2.5 - 20) μM BTSA1 and 1 μM staurosporine (STS) for 12 hr and cytosolic and mitochondrial fractions were separated and analyzed by western blot with anti-BAX antibody. Actin and VDAC immunoblot was used to confirm cytosolic and mitochondrial fractions. (**G**) Viability assays of indicated wild type, BAX KO, BAK KO and reconstituted BAX mutants MEF cell lines treated with 5 μM of BTSA1 for 24 hr. (**H**) Viability assays of wild type, BAX KO, BAK KO and reconstituted BAX mutants MEF cell lines treated with increasing concentrations of Navitoclax alone (blue curves) or in combination with 5 μM BTSA1 (red curves). IC_{50s} for Navitoclax alone (blue) or in combination with 5 μM BTSA1 (red) are indicated. Data represent mean ± SD (n=3) from two independent experiments or are representative of two independent experiments.

A

No.	Age	Sex	Cytogenetics	Mutations
1	67	F	48,XX,del(5)(q13q33),del(7)(q31q34),+8,add(9)(p22),+1	*TP53, DNMT3A*
2	59	M	Nml	*NRAS, U2AF1, CBL, GATA1*
3	37	F	+8	*FLT3 ITD*
4	65	F	-7	*DNMT3A, TET2, ASXL1, U2AF3*
5	61	M	-7	*ASXL1, RUNX1, EZH2*
6	83	F	+8	*EZH2, RUNX1, TET2, ASXL1, STAG2*

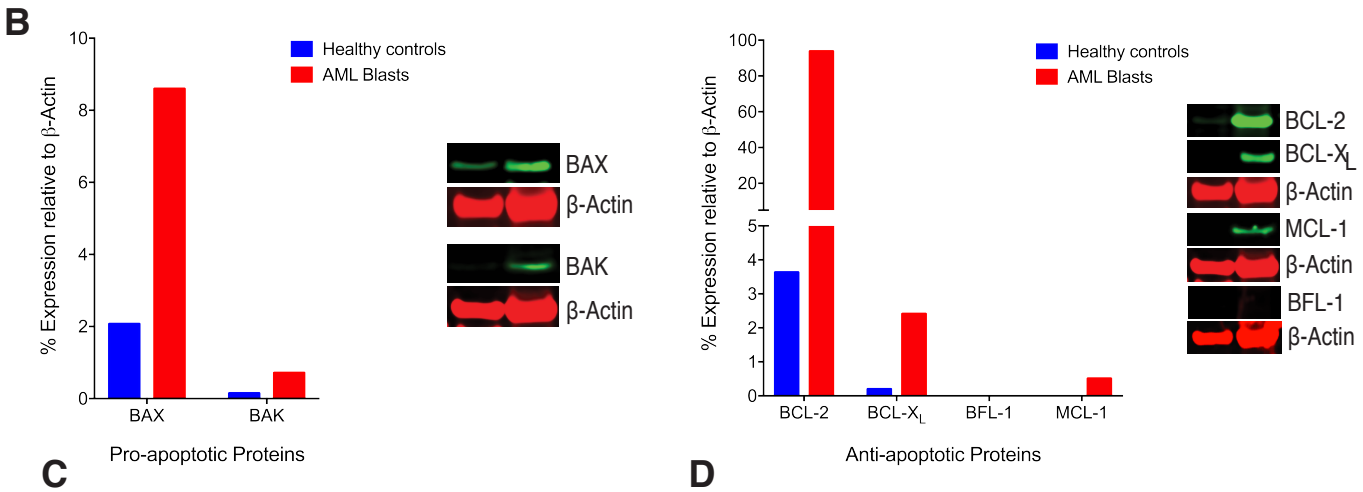

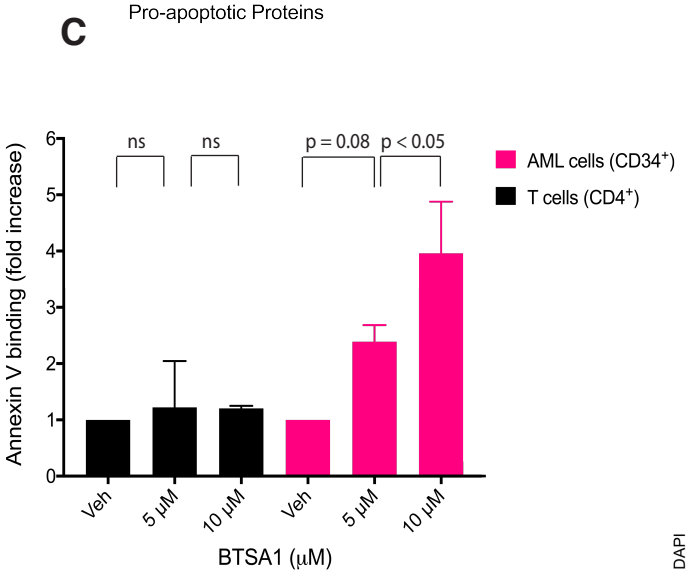

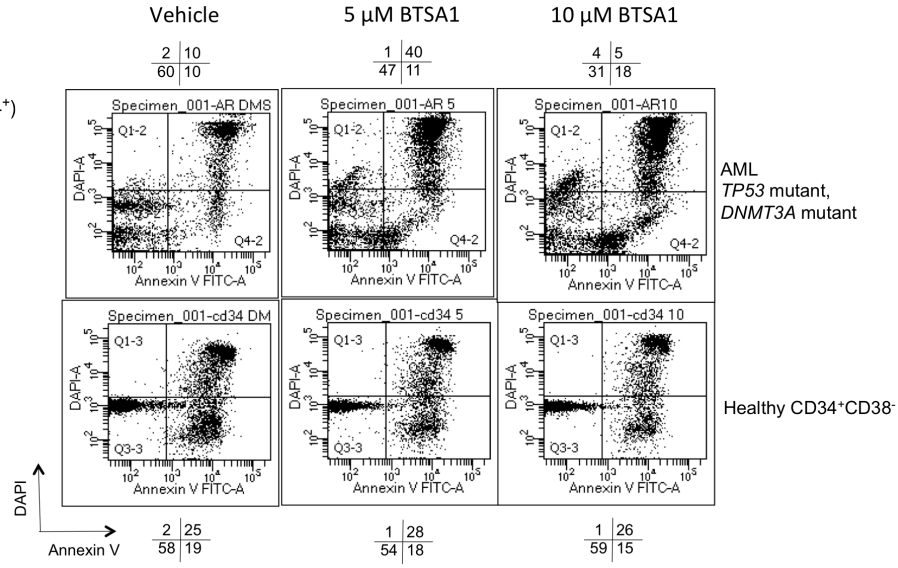

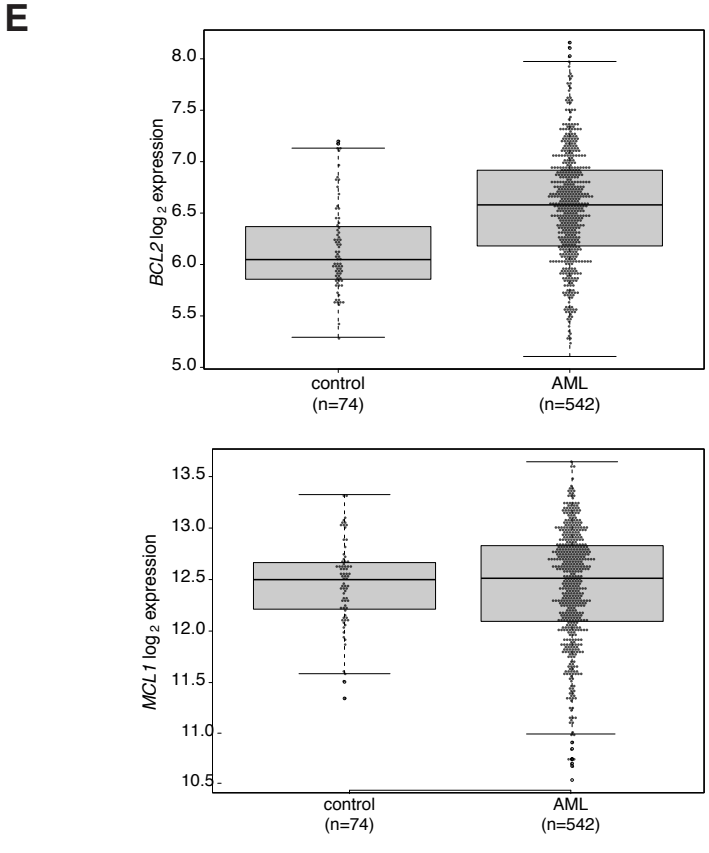

F

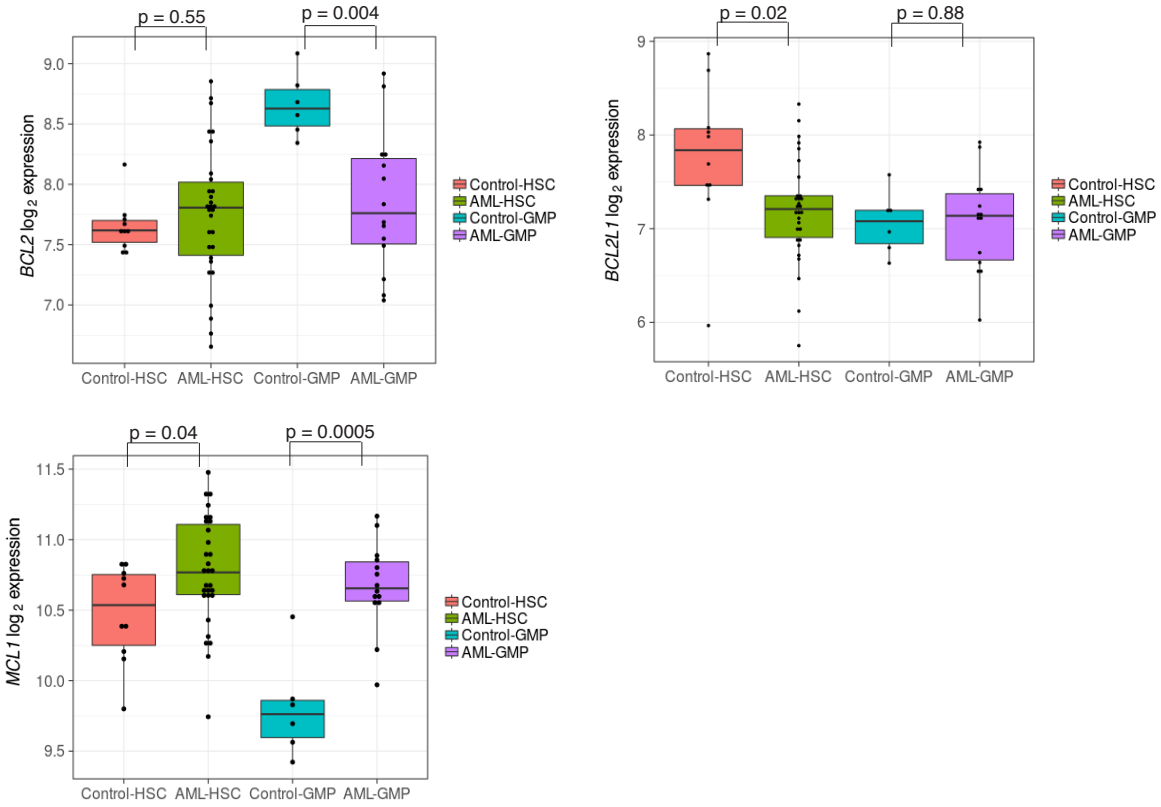
p = 0.55
p = 0.004
BCL2 log2 expression
Control-HSC
AML-HSC
Control-GMP
AML-GMP
p = 0.02
p = 0.88
BCL2L1 log2 expression
p = 0.04
p = 0.0005
MCL1 log2 expression

G

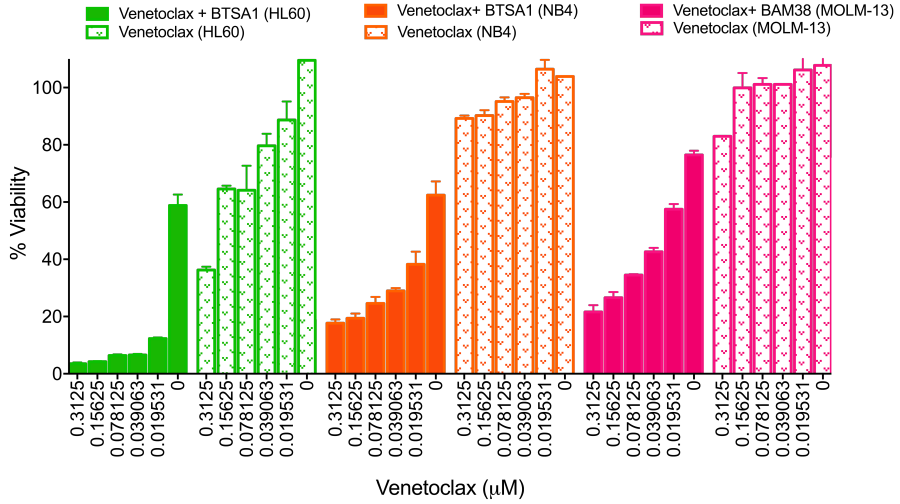
Venetoclax + BTSA1 (HL60)
Venetoclax (HL60)
Venetoclax+ BTSA1 (NB4)
Venetoclax (NB4)
Venetoclax+ BAM38 (MOLM-13)
Venetoclax (MOLM-13)
% Viability
Venetoclax (μM)

H

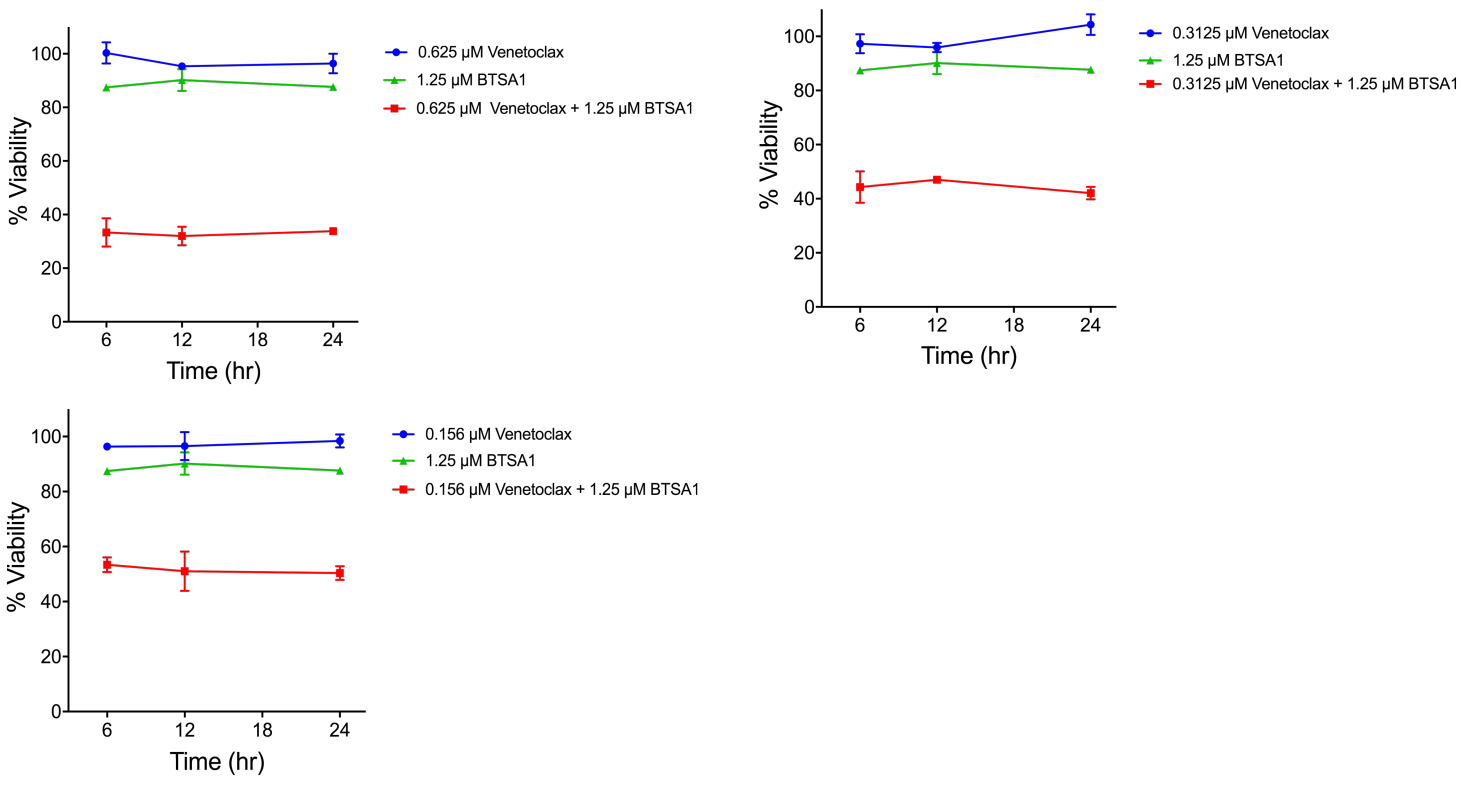
0.625 μM Venetoclax
1.25 μM BTSA1
0.625 μM Venetoclax + 1.25 μM BTSA1
0.3125 μM Venetoclax
0.3125 μM Venetoclax + 1.25 μM BTSA1
0.156 μM Venetoclax
0.156 μM Venetoclax + 1.25 μM BTSA1
% Viability
Time (hr)

Figure S5. Related to Figure 5.

Selective apoptosis induction by BTSA1 in primary samples from AML patients and the combination of BTSA1 with Venetoclax demonstrating significant synergy with fast kinetics. **(A)** Characteristics of AML patients. **(B)** Percent of BAX, BAK and anti-apoptotics (BCL-2, BCL-X_L and MCL-1) protein expression levels relative to Actin as measured by indicated quantitative IR fluorescence western analysis using human AML blasts and healthy control samples. **(C)** Apoptosis induction measured by Annexin V positivity in primary human AML blasts and healthy lymphocytes after 48 hr of BTSA1 treatment. **(D)** Flow cytometry data from gated leukemia $CD34^+CD38^-$ stem cell-enriched samples from one primary human AML sample (high risk *TP53* and *DNMT3A* mutant) and healthy control cells after 48 hours of treatment with BTSA1. **(E)** Boxplots showing comparison of *BCL2* (BCL-2) ($p = 1.5 \times 10^{-10}$), *BCL2L1* (BCL-X_L) ($p = 1.16 \times 10^{-5}$) and *MCL1* (MCL-1) ($p = 0.78$) mRNA expression in AML patient samples (n=542) and healthy controls (n=74). Line within box shows median expression, while edges of the box represent the 25th (bottom) and 75th percentile of expression (top). Whiskers indicate maximum and minimum values excluding outliers. **(F)** Boxplots showing comparison of *BCL2* (BCL-2), *BCL2L1* (BCL-X_L) and *MCL1* (MCL-1) mRNA expression in highly purified stem cells ($CD34^+CD38^-Lin^-$) and progenitor cell populations (Granulocytic Macrophage Progenitors, GMPs, ($Lin^-CD34^+CD38^+CD123^+CD45RA^+$) from AML patients and healthy controls. Line within box shows median expression, while edges of the box represent the 25th (bottom) and 75th percentile of expression (top). Whiskers indicate maximum and minimum values excluding outliers. **(G)** Viability assays of HL-60**,** NB4 and MOLM-13 cells treated with Venetoclax alone or in combination with 1.25 μM BTSA1 for 24 hr. **(H)** Viability assays of OCI-AML3 cells treated with (0.156 - 0.625) μM Venetoclax or 1.25 μM BTSA1 alone or their combination for 6, 12 and 24 hr. Data are presented as mean ± SD (n=3) of two independent experiments unless stated otherwise.

A

Time (hr)	Mean	SD
0.25	4068	737
0.5	3869	3338
1	9546	5264
2	12944	9970
4	14631	12437
8	15045	1444
24	3833	1124
48	1182	134

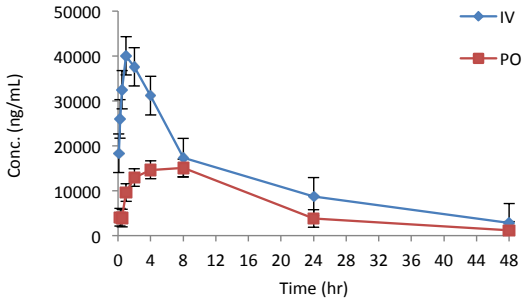

B

Time (hr)	Mean	SD
0.083	18332	7602
0.25	25983	4398
0.5	32463	8807
1	40003	1460
2	37555	4736
4	31146	6254
8	17325	4631
24	8673	1355
48	2814	752

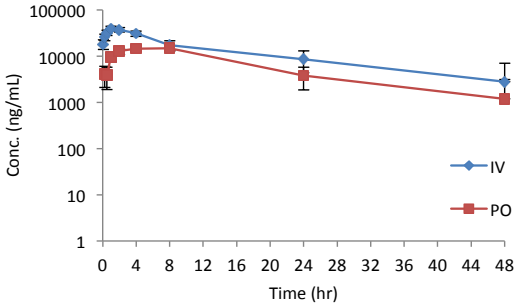

C

	$T_{1/2}$ (hr)	T_{max} (hr)	C_{max} (ng/mL)	AUC_{last} (hr*ng/mL)	AUC_{INF_obs} (hr*ng/mL)	CL_obs (mL/min/kg)	MRT_{INF_obs} (hr)	Vss_obs (mL/kg)	F%
p.o.	11	8	15045	288300	307235	-	17	-	
i.v.	15	-	-	557161	618929	0	20	323	52

p.o. use the last three times

Figure S6. Related to Figure 6.

Pharmacokinetic analysis of BTSA1 in mice. (A) Data and plots showing measured plasma concentration (ng/mL) of BTSA1 in ICR (CD-1) mice after oral administration of BTSA1 10 mg/Kg of body weight per mice at indicated times. Data are presented as mean ± SD (n=3). **(B)** Data and plot showing measured plasma concentration (ng/mL) of BTSA1 in ICR (CD-1) mice after intravenous administration of BTSA1 10 mg/Kg of body weight per mice at indicated times. Data are presented as mean ± SD (n=3). Plots for intravenous administration (IV) and oral administration (PO) levels are plotted in a linear and logarithmic y-axis scale in **A** and **B**, respectively. **(C)** Pharmacokinetic parameters for BTSA1: half-life ($T_{1/2}$), maximum concentration (C_{max}) at specific time T_{max}, area under the curve ($AUC_{0-\infty}$), clearance ($CL_{0-\infty}$), mean residence time ($MRT_{0-\infty}$), volume of distribution ($Vss_{0-\infty}$) and bioavailability (%F).

A

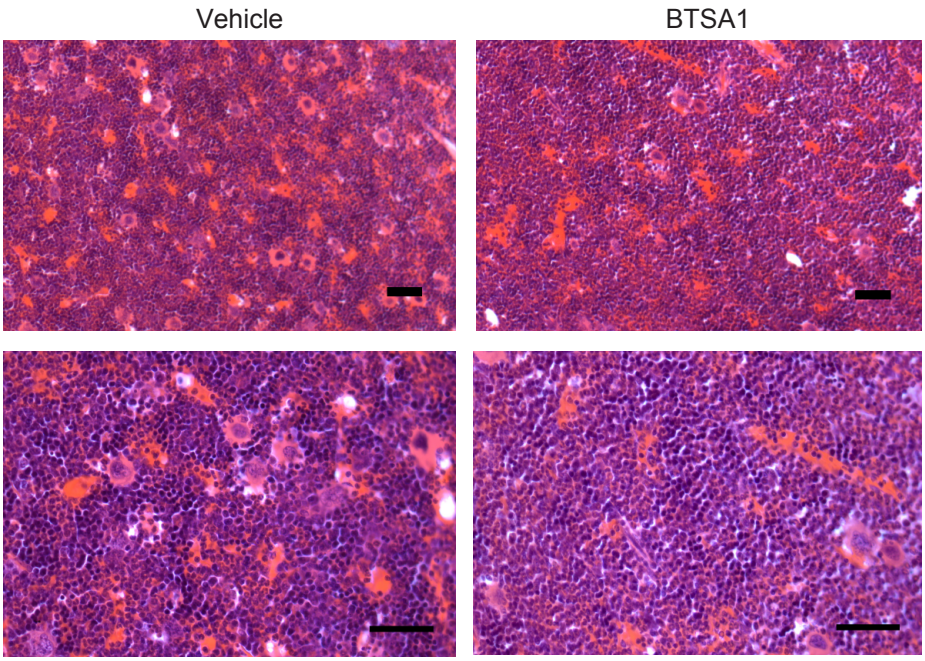
Vehicle
BTSA1

B

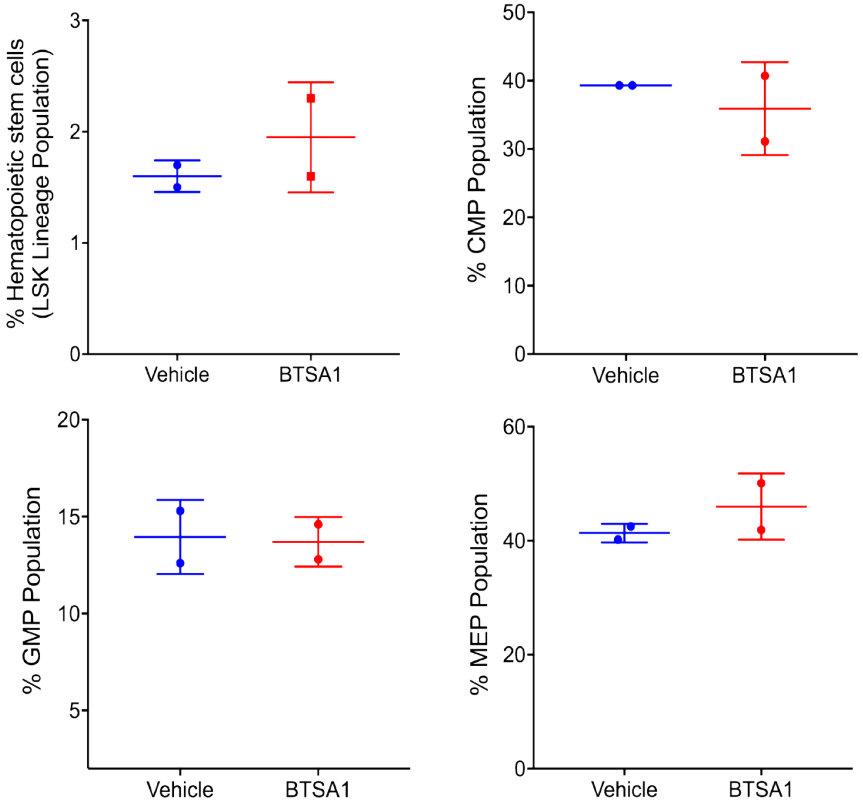
% Hematopoietic stem cells (LSK Lineage Population)
0
1
2
3
Vehicle
BTSA1
% CMP Population
0
10
20
30
40
50
Vehicle
BTSA1
% GMP Population
5
10
15
20
Vehicle
BTSA1
% MEP Population
0
20
40
60
Vehicle
BTSA1

Figure S7. Related to Figure 7.

BTSA1 is well tolerated *in vivo* and has no cytotoxic effect on hematopoietic stem cells and progenitors. (**A**) Representative tissue sections of bone morrow biopsies using Hematoxylin & Eosin staining from mice after treatment with vehicle and 15 mg/Kg BTSA1. Scale bar, 100 μm. (**B**) Bone marrow samples from vehicle and 15 mg/Kg BTSA1-treated cohorts were isolated for FACS analysis to evaluate hematopoietic stem cells and progenitor populations. Data are presented as mean ± SD (n=2).

Method S1. Related to STAR methods.
Chemical synthesis and analytical characterization for BTSA1, biotin-labeled BTSA1 and fluorescein-labeled BTSA1

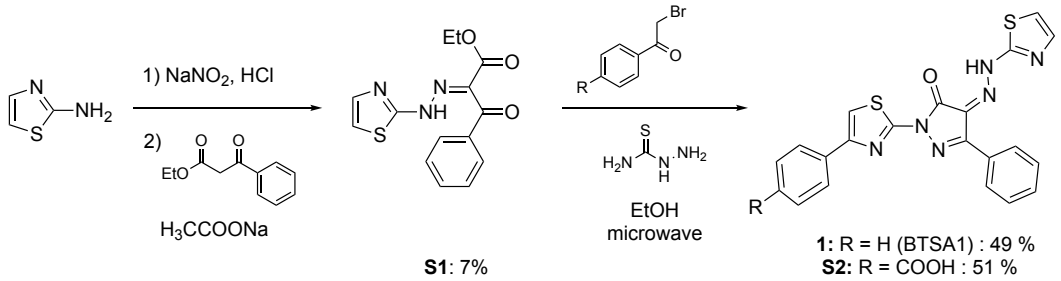

Scheme 1: Synthesis of BTSA1 (**1**) and the carboxylate-decorated analog **S2**. 2-Aminothiazole was diazotized and reacted *in situ* with ethyl 3-oxo-3-phenylpropanoate to give intermediate **S1**. **S1** was reacted with the respective 2-bromoacetophenone and hydrazinecarbothioamide under microwave conditions to give BTSA1 (**1**) or **S2**, respectively.

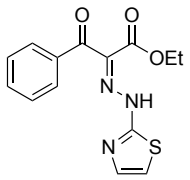

Synthesis of ethyl-3-oxo-3-phenyl-2-(2-(thiazol-2-yl)hydrazono)propanoate (S1):

To a solution of thiazol-2-amine (1.00 g, 9.99 mmol) in hydrochloric acid (3.94 mL, 130 mmol) and water (3.94 mL) at T ≤ –5 °C [*Note*: *internal thermometer, ice/NaCl cooling bath; additional cooling with N_2(l) droplets in the reaction vessel*] was added drop-wise a solution of sodium nitrite (689 mg, 9.99 mmol) in water (4.0 mL). The temperature was kept between –5 and 0 °C. The diazonium salt was formed as a clear, red-orange solution. After stirring this solution at the given temperature for another 10 min, it was added in small portions, down the thermometer, to a pre-cooled (0 °C) slurry of ethyl 3-oxo-3-phenylpropanoate (0.380 g, 2.00 mmol) and sodium acetate (12.3 g, 150 mmol) in ethanol (20.0 mL). The first drops caused a color change to dark green, later purple. After complete addition, the now dark brown slurry was stirred over night at RT. Water (ca. 300 mL) was added, the resulting mixture extracted with EtOAc (first 600 mL, then 2 × 150 mL). The combined organic layers were dried ($MgSO_4$), filtered and evaporated *in vacuo* to yield the crude product as dark purple resin.

After purification on the *Isco CombiFlash* (absorbed on ca. 15 g silica for loading; 80 g column; gradient 10→30 % EtOAc in hexanes), ethyl-3-oxo-3-phenyl-2-(2-(thiazol-2-yl)hydrazono)propanoate (**S1**; 1.06 g, 3.50 mmol, 7 %) was obtained as viscous red-orange oil (mixture of E/Z isomers).

TLC: R_f 0.24 (4:1, hex:EtOAc). **^{1}H-NMR** (600 MHz, $CDCl_3$):[1] δ 7.96 (dd, J = 8.2, 1.2 Hz, 2H), 7.61–7.58 (m, 1H), 7.48 (dd, J = 8.2, 7.6 Hz, 2H), 7.38 (d, J = 3.5 Hz, 1H), 6.83 (d, J = 3.5 Hz, 1H), 4.37 (q, J = 7.1 Hz, 2H), 1.32 (t, J = 7.1 Hz, 3H). **^{13}C-NMR** (151 MHz, $CDCl_3$):[1] δ 188.4, 167.0, 162.6, 140.0, 136.3, 133.3, 130.0, 128.3, 113.2, 62.2, 14.0. **ESI-MS** *m/z* (rel int): (pos) 325.9 ($[M+Na]^+$, 65), 303.9 ($[M+H]^+$, 100); (neg) 301.9 ($[M–H]^–$, 10).

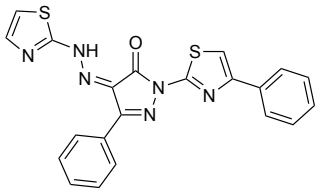

Synthesis of 5-phenyl-2-(4-phenylthiazol-2-yl)-4-(2-(thiazol-2-yl)hydrazono)-2,4-dihydro-3H-pyrazol-3-one (**1**): 2-Bromo-1-phenylethan-1-one (33.0 mg, 0.166 mmol) was weighed into a dry 10 mL microwave vessel, equipped with a rubber septum and stir bar, under an argon atmosphere. Dry ethanol (0.40 mL) was added at room temperature, upon which most of the starting material dissolved. To this mixture was added hydrazinecarbothioamide (15.1 mg, 0.166 mmol) neat, in one portion. The reaction mixture was stirred at room temperature for a 60 min. To the solution obtained from the first step, a solution of ethyl (Z)-3-oxo-3-phenyl-2-(2-(thiazol-2-yl)hydrazono)propanoate (**S1**; 50.0 mg, 0.165 mmol) in ethanol (1.10 mL) was added. The mixture was heated in the microwave (130 °C, 30 min). At the end of the reaction, a dark red-purple precipitate was submerged in a dark red solution. TLC analysis indicated full conversion of the starting material, MS analysis confirmed product mass. The precipitate was filtered in a Buchner filter, washed first with little cold EtOH (ca. 1 mL), then with diethyl ether (ca. 1 mL). The product was dried in high vacuum. (Z)-5-phenyl-2-(4-phenylthiazol-2-yl)-4-(2-(thiazol-2-yl)hydrazono)-2,4-dihydro-3H-pyrazol-3-one (**1**; 35 mg, 0.081 mmol, 49.3 % yield) was obtained as dark ruby-red solid. As an alternative to the microwave heating, conventional heating in an oil bath (80 °C, 4 h), afforded comparable results. The crude products after filtration are pure as judged by their ^{1}H and ^{13}C NMR spectra (aside of trace solvent). However, elemental analyses of crude samples as well as samples from commercial sources revealed remaining impurities (that can not be explained by trace solvent remainders). The crude product can be additionally purified by column chromatography (silica gel, gradient of MeOH in CH_2Cl_2), or crystallization from 1,4-dioxane. Only the latter afforded material that gives satisfactory data in the elemental analysis (calculated: C: 58.59; H: 3.28; N: 19.52; S: 14.89; found: C: 58.52; H: 3.18; N: 19.17; S: 14.63). However, all samples showed very similar activities well within the error margins.

TLC: R_f 0.75 (19:1, CH_2Cl_2/MeOH); 0.11 (1:1, hex:EtOAc). **^{1}H-NMR** (600 MHz, dmso-d_6): δ 8.16 (d, J = 7.0 Hz, 2H), 7.99 (dd, J = 8.2, 1.1 Hz, 2H), 7.83 (s, 1H), 7.71 (d, J = 4.0 Hz, 1H), 7.57–7.51 (m, 3H), 7.46 (t, J = 7.7 Hz, 2H), 7.37–7.34 (m, 2H). **^{13}C-NMR** (151 MHz, dmso-d_6): δ 179.0, 154.7, 152.9, 149.9, 149.0, 134.1, 131.9, 130.5, 129.9(6), 129.9(2), 128.7, 128.5, 127.9(7), 127.9(6), 125.9, 114.0, 109.0. **ESI-MS** *m/z* (rel int): (pos) 883.2

[1] Signals of major isomer given.

([2M+Na]$^+$, 35), 452.9 ([M+Na]$^+$,20), 430.9 ([M+H]$^+$,60), 168.8 (100) (neg) 429.0 ([M–H]$^-$, 100). **HRMS** calculated for $C_{21}H_{15}N_6OS_2$ (M+H): 431.0743, found: 431.0767.

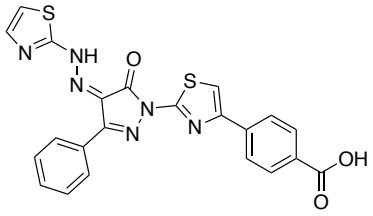

Synthesis of 4-(2-(5-oxo-3-phenyl-4-(2-(thiazol-2-yl)hydrazono)-4,5-dihydro-1H-pyrazol-1-yl)thiazol-4-yl)benzoic acid (**S2**): Synthesized as described for **1** using 4-(2-bromoacetyl)benzoic acid (40.0 mg, 0.165 mmol) instead of 2-bromo-1-phenylethan-1-one. **S2** was obtained as red solid (40.0 mg, 0.084 mmol, 51 %). The product contained about 6% of the corresponding ethyl ester as an impurity, and was used in the next step without further purification.

Note: microwave conditions are required for this substrate, as no complete conversion was obtained using conventional heating.

TLC: R_f 0.30 (19:1, CH_2Cl_2/MeOH). **^{1}H-NMR** (600 MHz, dmso-d_6): δ 8.15 (s, 2H), 8.11 (d, J = 8.5 Hz, 2H), 8.03 (m, 3H), 7.72 (d, J = 4.0 Hz, 1H), 7.58–7.52 (m, 3H), 7.36 (d, J = 4.0 Hz, 1H). **^{13}C-NMR** (151 MHz, dmso-d_6): δ 179.8, 167.5, 155.3, 153.4, 149.7, 149.3, 138.4, 132.3, 131.0, 130.4(1), 130.4(0), 130.3, 130.2, 129.0, 128.5, 126.4, 114.5, 111.8. **ESI-MS** *m/z* (rel int): (473.0 ([M–H]$^-$, 100). **HRMS** calculated for $C_{22}H_{13}N_6O_3S_2$ (M–H) 473.0496, found: 473.0512.

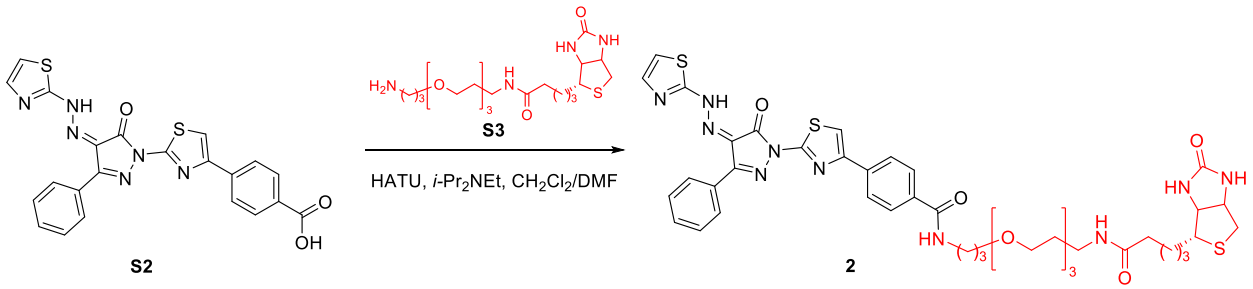

Scheme 2: Synthesis of the biotin-labeled BTSA1-analog **2**. The carboxylic acid **S2** was coupled with the known Biotin tag, N-(3-(2-(2-(3-aminopropoxy)ethoxy)ethoxy)propyl)5-((4S)-2-oxohexahydro-1H-thieno[3,4-d]imidazol-4-yl)pentanamide (**S3**) using a standard HATU protocol.

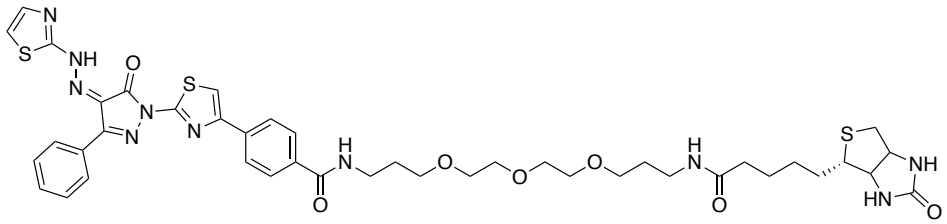

Synthesis of N-(15-oxo-19-((4R)-2-oxohexahydro-1H-thieno[3,4-d]imidazol-4-yl)-4,7,10-trioxa-14-azanonadecyl)-4-(2-(5-oxo-3-phenyl-4-(2-(thiazol-2-yl)hydrazono)-4,5-dihydro-1Hpyrazol-1-yl)thiazol-4-yl)benzamide (**2**): 4-(2-(5-Oxo-3-phenyl-4-(2-(thiazol-2-yl)hydrazono)-4,5-dihydro-1H-pyrazol-1-yl)thiazol-4-yl)benzoic acid (**S2**; 15.0 mg, 0.032 mmol) was dissolved in dry dichloromethane (500 µL). *N*-Ethyl-*N*-isopropylpropan-2-amine (27 µL, 0.16 mmol) was added. followed by HATU (13.2 mg, 0.035 mmol). Dry dimethylformamide (200 µL) was added to improve solubility. After 25 min, N-(3-(2-(2-(3-aminopropoxy)ethoxy)ethoxy)propyl)-5-((4S)-2-oxohexahydro-1H-thieno[3,4-d]imidazol-4-yl)pentanamide (15.5 mg, 0.035 mmol) in dimethylformamide (500 µL) was added at room temperature. LC-MS and TLC anaylsis of a reaction aliquot (micro-workup: satd. aq. $NaHCO_3$/EtOAc) after 2 h indicated full conversion. The solvent was evaporated on the rotary evaporator, then by vacuum destillation. The residue was dissolved in dichloromethane/MeOH, absorbed on silica gel and subjected to column chromatography (silica; *1731-mix*[2]). N-(15-oxo-19-((4S)-2-oxohexahydro-1H-thieno[3,4-d]imidazol-4-yl)-4,7,10-trioxa-14-azanonadecyl)-4-(2-(5-oxo-3-phenyl-4-(2-(thiazol-2-yl)hydrazono)-4,5-dihydro-1H-pyrazol-1-yl)thiazol-4-yl)benzamide (**2**; 12.9 mg, 0.014 mmol, 45 %) was obtained as bright orange-red solid in form of an ammonium salt (as identified by ^{1}H-NMR).

TLC: R_f 0.47 (17:3:1, EtOAc/MeOH/NH_4OH). **^{1}H-NMR** (600 MHz, dmso-d_6): δ 8.49 (t, J = 5.5 Hz, 1H), 8.21 (dd, J = 6.1, 0.6 Hz, 2H), 8.07 (d, J = 8.4 Hz, 2H), 7.92 (d, J = 8.4 Hz, 2H), 7.84 (s, 1H), 7.73 (dd, J = 7.3, 3.8 Hz, 1H), 7.65 (d, J = 3.2 Hz, 1H), 7.51–7.49 (m, 2H), 7.44 (t, J = 7.3 Hz, 1H), 7.25 (d, J = 3.2 Hz, 1H), 6.41 (s, 1H), 6.34 (s, 1H), 4.28 (dd, J = 7.4, 5.2 Hz, 1H), 4.11 (ddd, J = 7.4, 4.8, 2.1 Hz, 1H), 3.55–3.50 (m, 6H), 3.49–3.46 (m, 4H), 3.38 (t, J = 6.7 Hz, 2H), 3.34 (t, J = 6.7 Hz, 2H), 3.09–3.05 (m, 3H), 2.80 (dd, J = 12.4, 5.2 Hz, 1H), 2.56 (d, J = 12.4 Hz, 1H), 2.04 (dd, J = 9.7, 5.2 Hz, 2H), 1.78 (quintet, J = 6.6 Hz, 2H), 1.60 (dd, J = 8.6, 4.9 Hz, 3H), 1.48 (t, J = 7.3 Hz, 3H), 1.23 (s, 2H). **^{13}C-NMR** (151 MHz, dmso-d_6): δ 182.7, 171.9, 165.8, 162.7, 155.4, 152.9, 149.8, 148.4, 141.2, 136.9, 133.4, 132.8, 128.6, 128.1(2), 128.0(5), 127.6, 125.5, 121.9, 115.4, 109.6, 69.8(0), 69.7(7), 69.6, 69.5, 68.3, 68.1, 61.0, 59.2, 55.4, 39.8 (concealed by the solvent signal, identified by HSQC experiment), 36.7, 35.7, 35.2, 29.4 (2 carbons, as confirmed by HSQC experiment), 28.2, 28.0, 25.3. **ESI-MS** *m/z* (rel int): (pos) 903.4 ([M+H]$^+$, 15), 545.3 (85), 405.1 (100), 295,2 (50); (neg) 901.5 ([M–H]$^-$, 15), (312.8, 30). **HRMS** calculated for $C_{42}H_{49}N_{10}O_7S_3$ (M–H): 901.2953, found: 901.3000.

[2] *1731-mix* = 17:3:1 EtOAc:MeOH:H_2O.

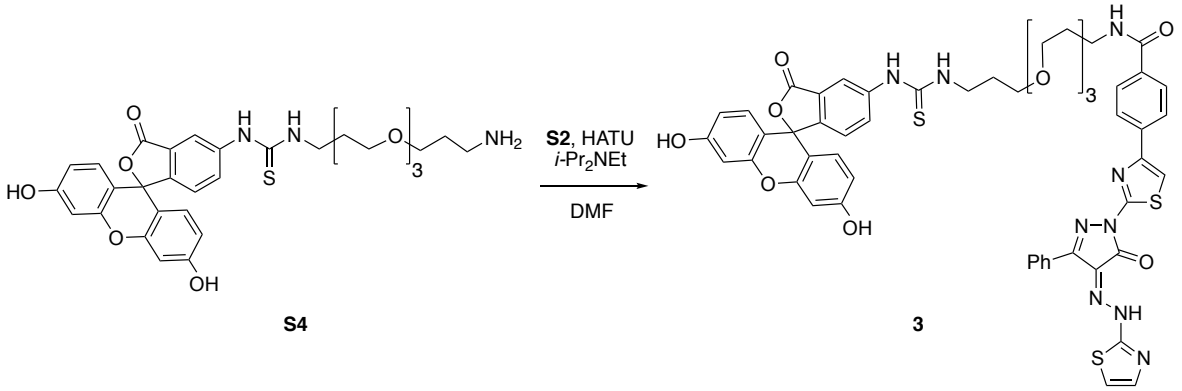

Scheme 3: Synthesis of fluorescein-labeled BTSA1 **3.** The PEG linker-equipped FitC derivative **S4** (synthesized according to literature) was attached to the carboxylic acid of BTSA1-analog **S2** utilizing standard HATU coupling chemistry. HATU = 1-[Bis(dimethylamino)methylene]-1H-1,2,3-triazolo[4,5-b]pyridinium 3-oxide hexafluorophosphate; DMF = *N,N*-dimethylformamide.

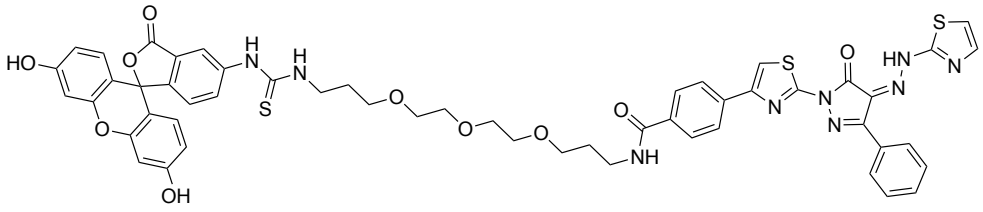

Synthesis of *N*-(1-((3',6'-dihydroxy-3-oxo-3*H*-spiro[isobenzofuran-1,9'-xanthen]-5-yl)amino)-1-thioxo-6,9,12-trioxa-2-azapentadecan-15-yl)-4-(2-(5-oxo-3-phenyl-4-(2-(thiazol-2-yl)hydrazineylidene)-4,5-dihydro-1*H*-pyrazol-1-yl)thiazol-4-yl)benzamide (3): In a dry conical tube with stir bar and septum, S**2** (22.0 mg, 46.0 μmol) and HATU (19.4 mg, 50.0 μmol, 1.10 equiv) were dissolved in dry *N,N*-dimethylformamide (DMF; 1.00 mL). *Hunig*'s Base (40.5 μL, 0.232 mmol, 5.00 equiv) was added at RT and the mixture was stirred for 30 min. 1-(3-(2-(2-(3-aminopropoxy)ethoxy)ethoxy)propyl)-3(3',6'dihydroxy-3-oxo-3H-spiro[isobenzofuran-1,9'-xanthen]-5-yl)thiourea (**S4**; 28.3 mg, 46.0 μmol, 1.00 equiv) in dry DMF (4.00 mL) was added at RT, and the resulting mixture was stirred at RT in the dark. After 18 h, MS analysis of a reaction aliquot indicated product formation (TLC analysis was nconclusive). The solvent was evaporated *in vacuo*. Purification on the *Isco CombiFlash* (silica gel, *1731-mix*[2] in EtOAc, 40 % → 85 %) afforded *N*-(1-((3',6'-dihydroxy-3-oxo-3*H*-spiro[isobenzofuran-1,9'-xanthen]-5-yl)amino)-1-thioxo-6,9,12-trioxa-2-azapentadecan-15-yl)-4-(2-(5-oxo-3-phenyl-4-(2-(thiazol-2-yl)hydrazineylidene)-4,5-dihydro-1*H*-pyrazol-1-yl)thiazol-4-yl)-benzamide (**3**; 13.2 mg, 12 μmol, 27 %,. >90% purity as estimated based on the ^{1}H-NMR trace) as light red solid

TLC: R_f = 0.28 (1:1, EtOAc:*1731-mix*). **^{1}H-NMR** (600 MHz, dmso-d_6): δ 10.13 (s, 2H), 9.97 (s, 1H), 8.50 (t, *J* = 5.6 Hz, 1H), 8.25–8.18 (m, 3H), 8.13 (s, 1H), 8.07 (d, *J* = 8.4 Hz, 2H), 7.92 (d, *J* = 8.4 Hz, 2H), 7.82 (s, 1H), 7.73 (d, *J*

= 6.7 Hz, 1H), 7.64 (d, *J* = 3.1 Hz, 1H), 7.49 (t, *J* = 7.5 Hz, 2H), 7.42 (t, *J* = 7.3 Hz, 1H), 7.24 (d, *J* = 3.5 Hz, 1H), 7.17 (d, *J* = 8.3 Hz, 1H), 6.66 (s, 2H), 6.60 (d, *J* = 8.7 Hz, 2H), 6.56 (dd, *J* = 8.7, 2.0 Hz, 2H), 3.55–3.47 (m, 16H), 1.84–1.76 (m, 4H). **^{13}C-NMR** (151 MHz, dmso-d_6): δ 182.8, 180.4, 168.6, 165.9, 159.5, 155.4, 153.0, 151.9, 149.9, 148.4, 141.5, 141.3, 136.9, 133.4, 132.9, 129.4, 129.1, 128.5, 128.1, 128.1, 127.6, 125.6, 124.1, 121.7, 116.5, 115.5, 112.7, 109.8, 109.6, 102.2, 69.8(2), 69.7(6), 69.6 (2 carbons, based on signal shape and HSQC correlation[3]), 68.4, 68.2, 41.5, 36.7, 29.4, 28.6. **HRMS** (for $C_{53}H_{48}N_9O_{10}S_3$): calculated: 1066.2681; found: 1066.2719.

[3] Based on the HSQC data, an unambiguous assignment was not possible, due to the overlap of the corresponding signals in the proton spectrum. However, the group of 3 signals at around 69 ppm, based on the signals seen in the proton spectrum can be identified as the four ethylene glycol methylene groups from the PEG linker. The signal at 69.6 ppm appears to have a much broader base and higher amplitude than the neighboring signals at 69.82 and 69.76 ppm, respectively, suggesting that it is actually two overlapping methylene signals.

^{1}H and ^{13}C NMR Spectra of 1 in dmso-d_6

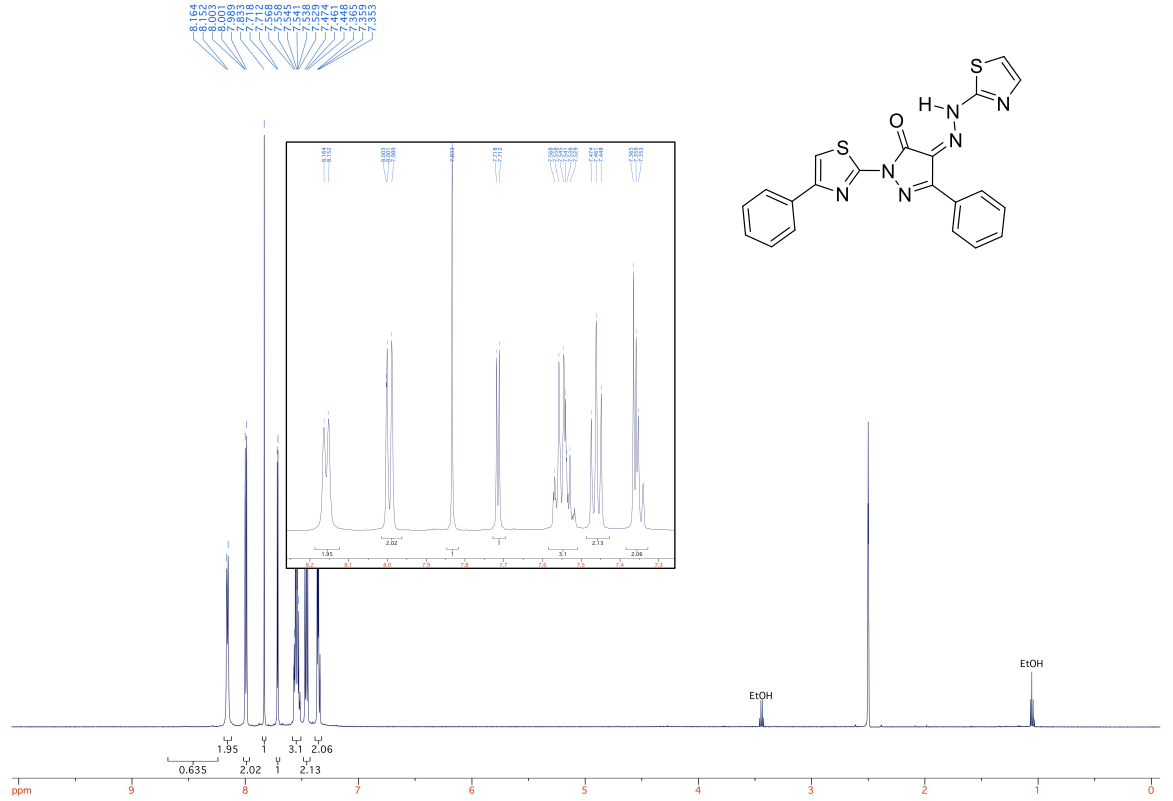

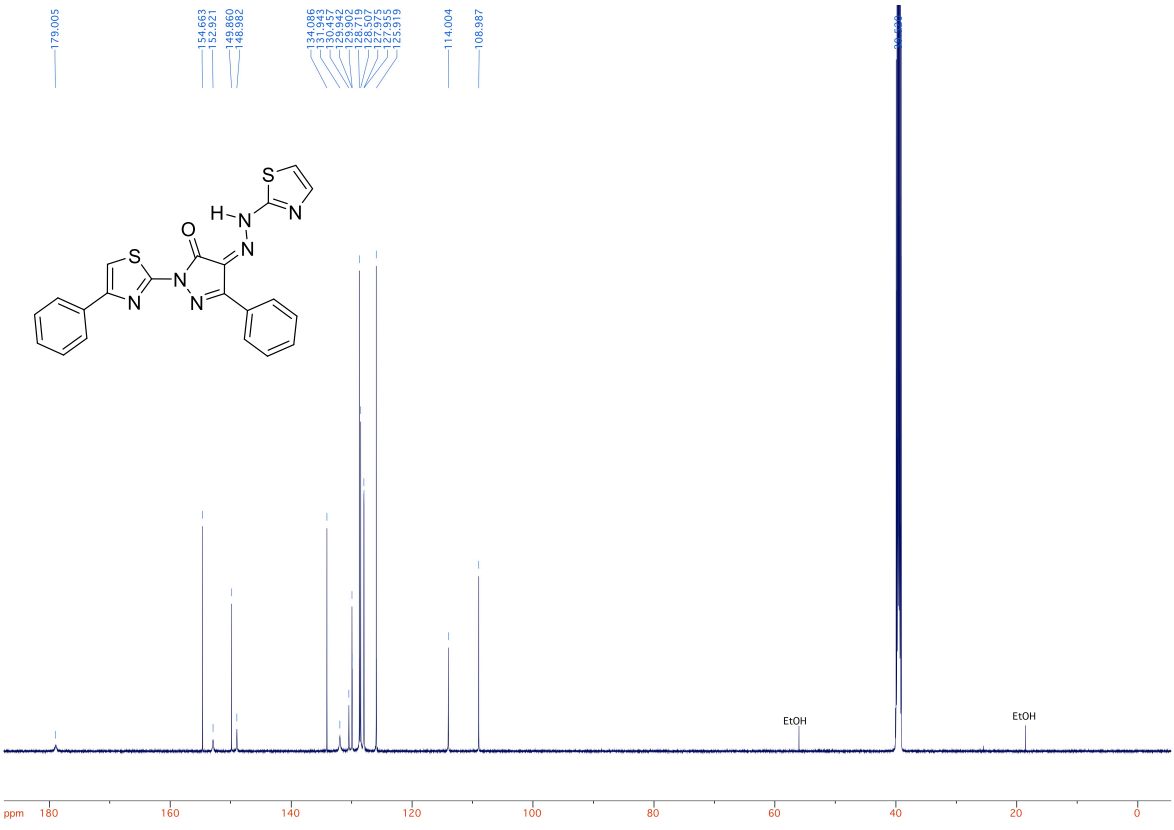

^{1}H and ^{13}C NMR Spectra of 2 in dmso-d_6

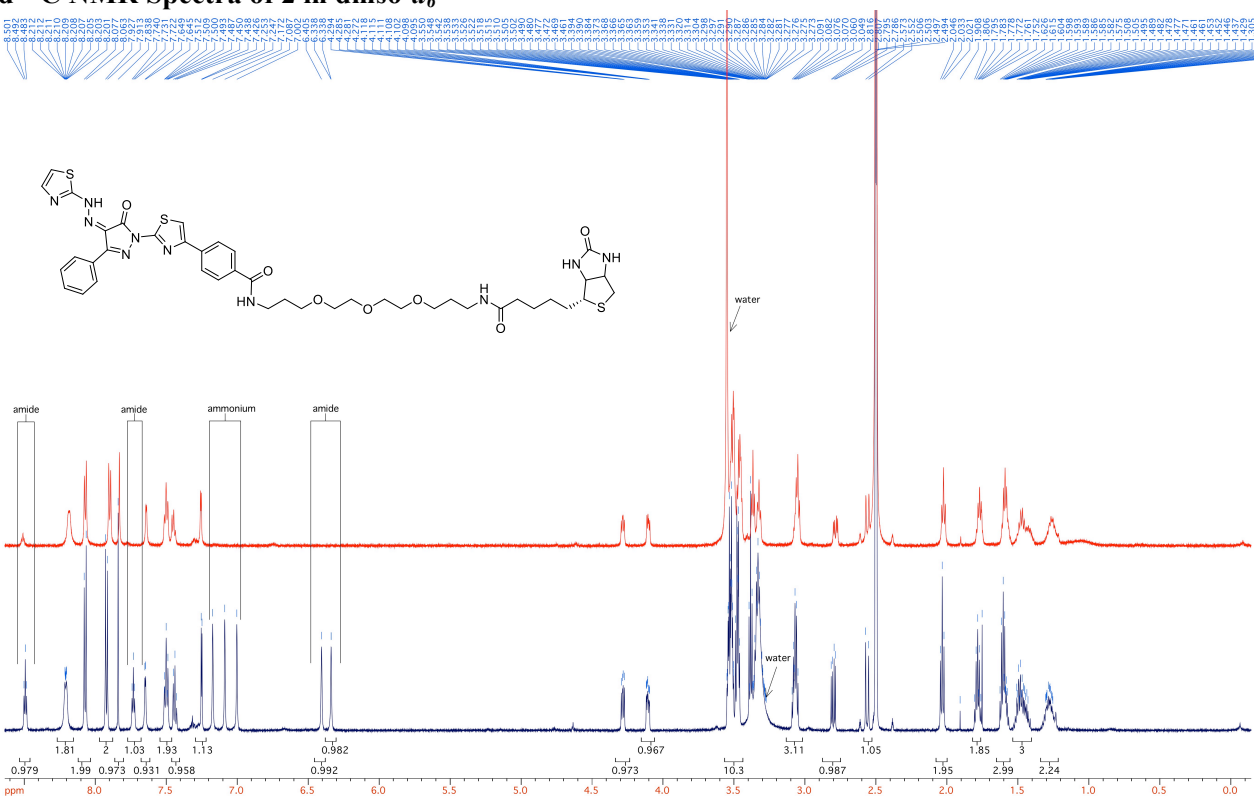

^{1}H-NMR of 1) a sample in dmso-d_6 (blue trace); 2) the same sample after addition of ca 50µL D_2O to resolve a signal overlap with H_2O in dmso-d_6 by shifting the water signal and to visualize exchangeable protons (red trace).

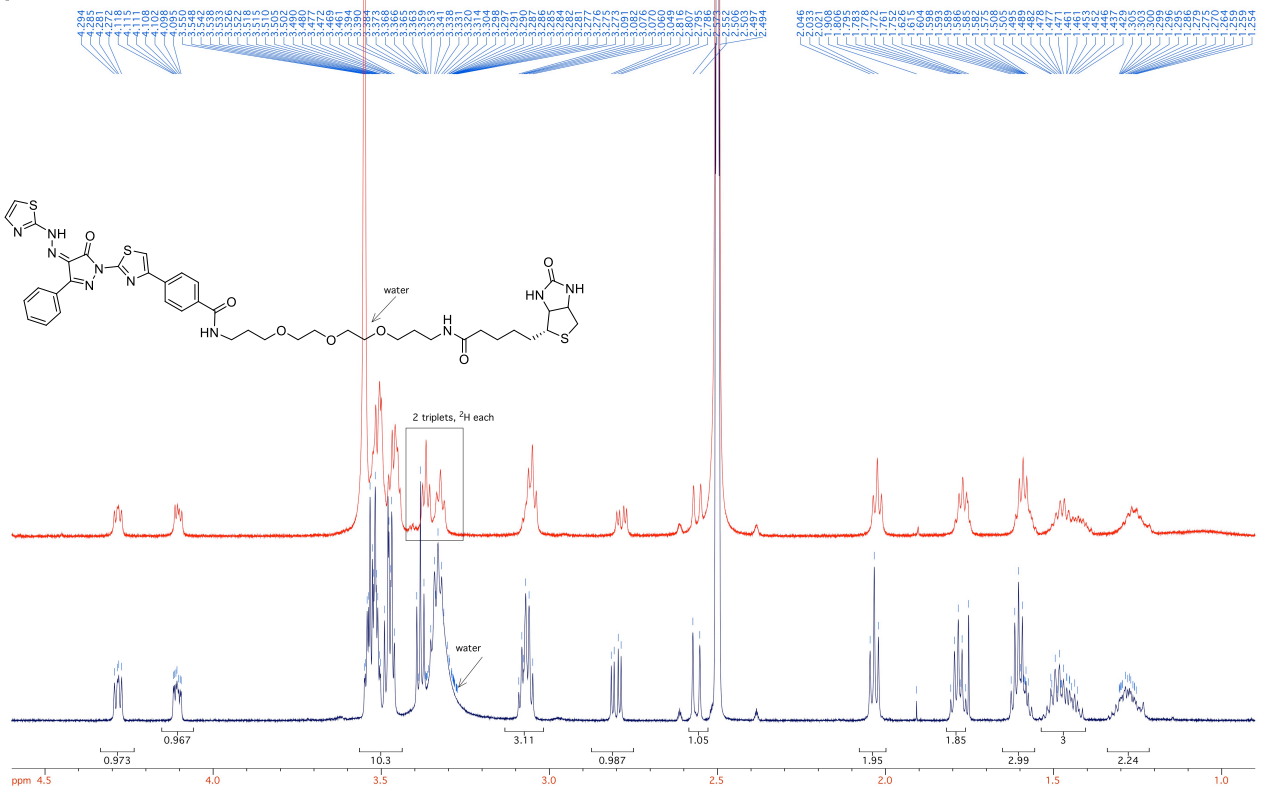

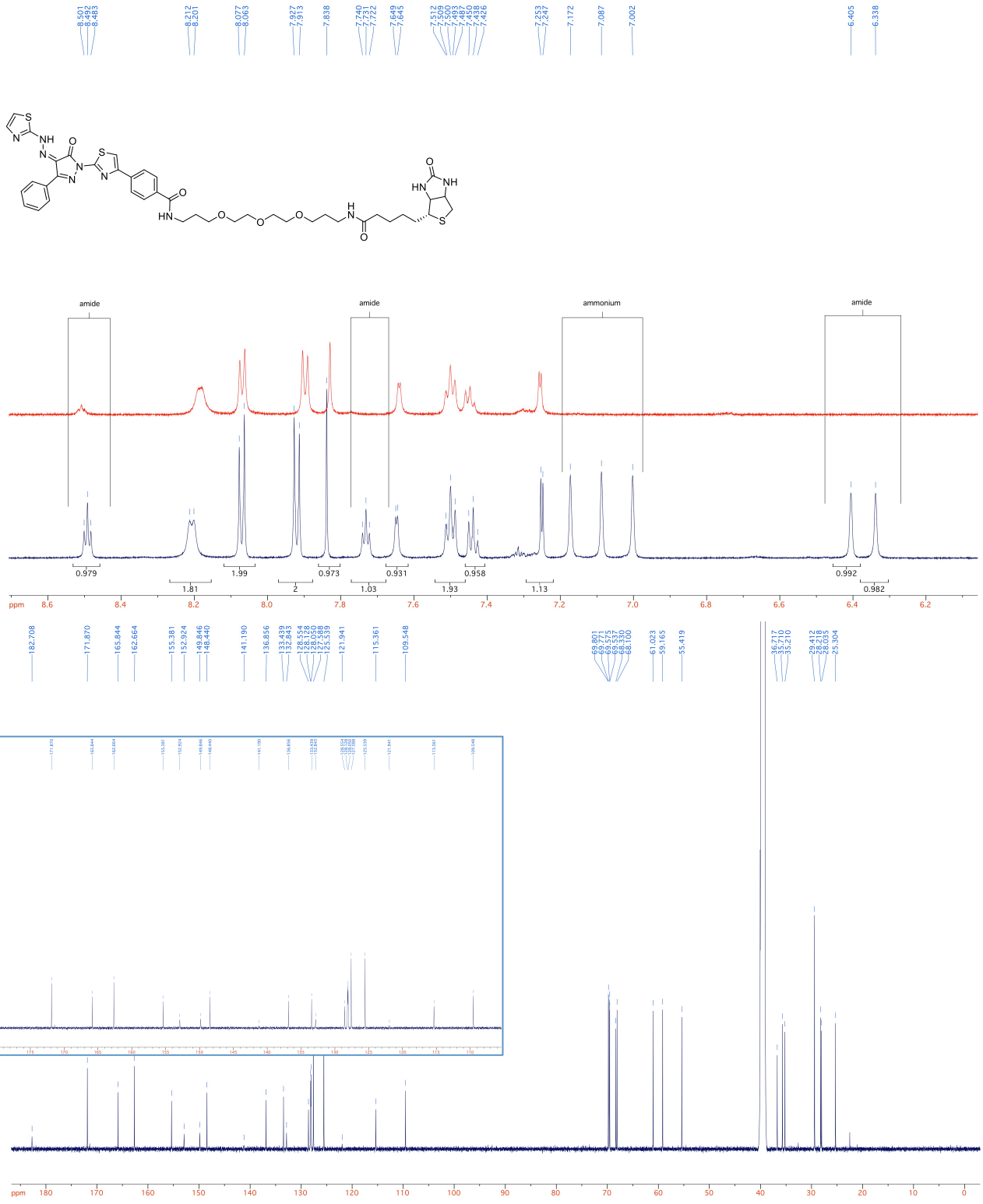
8.501
8.492
8.483
8.212
8.201
8.077
8.063
7.927
7.913
7.838
7.740
7.731
7.722
7.649
7.645
7.512
7.509
7.500
7.493
7.487
7.450
7.438
7.426
7.253
7.247
7.172
7.087
7.002
6.405
6.338
amide
amide
ammonium
amide
0.979
1.81
1.99
2
0.973
1.03
0.931
1.93
0.958
1.13
0.992
0.982
ppm
182.708
171.870
165.844
162.664
155.381
152.924
149.846
148.440
141.190
136.856
133.439
132.843
128.554
128.178
128.000
127.588
125.539
121.941
115.361
109.548
69.801
69.771
69.577
69.537
68.330
68.100
61.023
59.165
55.419
36.717
35.710
35.210
29.412
28.218
28.035
25.304
ppm

^{1}H and ^{13}C NMR Spectra of 3 in dmso-d_6